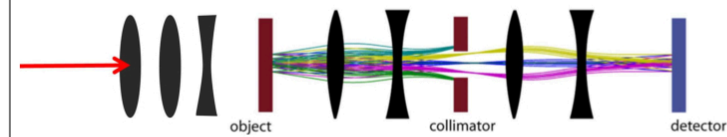


## ABSTRACT

Proton radiography could serve as a real-time imaging modality for proton therapy, facilitating more patient accurate positioning and further tightening the margins on the Planning Treatment Volume. In this project, the 800-MeV proton radiography (pRad) system at the Los Alamos Neutron Science Center (LANSCE) is modeled using the TOL for Particle Simulation (TOPAS) [1]. The system modeled here produces quality radiographs using a full proton field combined with a magnetic-lens refocusing system. All components of the LANSCE pRad system were modeled as well as several phantoms used in PET (Positron Emission Tomography) and SPECT (Single Photon Emission Computed Tomography) quality assurance. Water, gallium-68, and gold were placed in these phantoms to determine which provided the highest contrast for proton imaging; both <sup>68</sup>Ga and gold would be sufficient contrast agents while water (representing tissue without some contrast agent) would not provide enough contrast. TOPAS employs a hierarchy of text files that allows users to easily place their own phantom into the pRad system and determine the viability of their experiment, indicating it could be easily deployed as an open source tool for the medical community to evaluate instantaneous, high-energy proton radiography.

## INTRODUCTION

Proton radiography based on a magnetic lens system [2,3] provides an instantaneous measure of proton stopping power that could be used to adjust a patient's treatment plan in real-time to accommodate daily changes in anatomy [4]. The quadrupole-based magnetic lens system focuses the protons into a downstream image. A Fourier plane in the lens maps the angle of proton scatter to position. A collimator placed therein attenuates transmission, making changes in transmission highly sensitive to changes in thickness.



**Figure 1:** The proton beam trajectory for the LANSCE proton radiography system. After the object, the beam becomes scattered. The lenses sort the beam scattering by angle at the Fourier plane, where a collimator removes the most highly scattered portions of the beam. The remaining beam is then focused on the detector.

The resolution of this system is sensitive to: 1. the spread in energies of transmitted protons and 2. the multiple-Coulomb scattering accumulated after a proton has traversed a patient. Instantaneous proton radiography is better suited to operate at higher proton energies and mitigates system blur by minimizing both scatter (equation 1) [5] and dE/E, the variation in proton exit energy from the nominal focus energy of the lens.

Currently, a patient's proton stopping power map is calculated from an X-ray CT with an error of  $\pm 2\%$  [6]. Proton radiography directly measures proton stopping power: transmission is converted to water equivalent path length (WEPL) according to (1).  $\theta_0$  defines the Gaussian distribution of the proton angular distribution, defined in (2). Using the known nuclear attenuation coefficients for water, the measured transmission is converted to WEPL.

$$T = e^{-\frac{x}{\lambda}} [1 - e^{-\left(\frac{\theta_c^2}{\theta_0^2}\right)}] \quad (1)$$

$$\theta_0 = \frac{13.6 \text{ MeV}}{\beta p} \sqrt{\frac{x}{x_0}} [1 + 0.038 \ln\left(\frac{x}{x_0}\right)] \quad (2)$$

**Equations (1) and (2).**  $x$  is the density,  $\lambda$  is the nuclear attenuation coefficient, and  $\theta_c$  is the collimation cut angle;  $\beta$  is the relativistic velocity,  $p$  is momentum, and  $x_0$  is the radiation length

Here, the 800-MeV proton radiography system at LANSCE is modeled using the TOL for Particle Simulation (TOPAS) [1]. TOPAS incorporates the physics of Geant4 in a user friendly package for Monte Carlo simulations of proton and heavy ion therapy treatments easy to deploy as open source tool for the medical community.

## MATERIALS AND METHODS

### Proton Radiography System

The lens-based pRad system was designed using differential algebraic-based beamline design code COSY INFINITY [7]. To replicate the proton beam at LANSCE,  $10^7$  particles were used per simulation, delivered with Gaussian spread of  $\sigma = 0.85$  cm.

The pRad system begins with a tantalum diffuser foil, placed where the beam is at a double-waist. This diffuses the beam, which is formed within three quadrupole magnets to provide the position and angle matching conditions that enable a Fourier plane within the downstream lens system. Phantoms are imaged through a 'lens' of four quadrupoles, modeled as vacuum cylinders with electro-magnetic field gradients. The  $15 \times 15 \times 0.2$  cm<sup>3</sup> LYSO detector is divided into  $1500 \times 1500 \times 1$  histogram bins and the energy deposited in each bin scored.

Simulations took approximately 24 hours and varied depending on the collimator used. An intensity image (energy per bin) was generated in Python. Flat fields were acquired as an image with no object present. Images were flattened by dividing the phantom image by the flat field. Visibility was optimized in ImageJ.

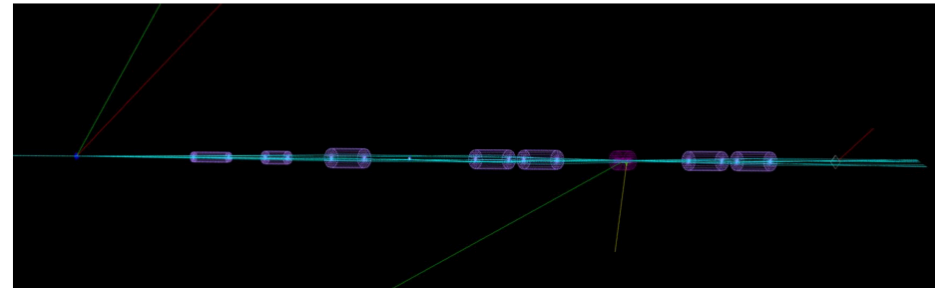


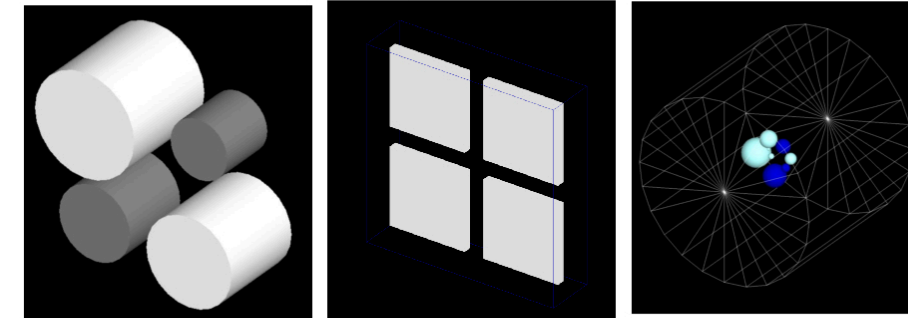
**Figure 2:** A bird's-eye view of the pRad system with a small number of protons. On the far left is the tantalum diffuser, followed by three beam-forming quadrupoles. After the object plane, two sets of two quadrupoles are separated by a collimator (dark purple) before reaching the detector at the far right. The teal lines are proton trajectories, while the other lines are scattered particles such as electrons, neutrons, or photons.

### Phantoms

Various phantoms were modeled to assess the system resolution and amount of contrast agent needed to produce an image. They were designed to replicate PET/SPECT quality assurance phantoms.

Phantom	Description	Dimensions	Material	Density
Jaszczak sphere phantom	Water spheres in a vacuum cylinder	Diameters: 3.1, 6.3, 9.5, 12.7, 15.9, 19.1, 25.4, 31.8 mm	Water, Gold, or <sup>68</sup> Ga	Water: 1.000 g/cm <sup>3</sup> Gold: 19.32 g/cm <sup>3</sup> <sup>68</sup> Ga: 5.91 g/cm <sup>3</sup>
Cylinder Phantom	Water cylinders	Diameters: 2, 2.5, 3, 3.5 cm; length: 3.5 cm	Water	1.000 g/cm <sup>3</sup>
Box Phantom	Lead boxes in a vacuum box	Box length: 2 cm x, 2 cm 7, 0.2 cm z	Lead	11.35 g/cm <sup>3</sup>

**Figure 3:** Imaging phantoms used in the proton radiography system. In medical imaging, they are used to assess things such as resolution and contrast. From left to right: Jaszczak phantom, cylinder phantom, and box phantom. Specifications are provided in Table 1.



## RESULTS

### Effect of Collimator

The purpose of a collimator is to provide a predictable and quantifiable way in which transmission scales with water equivalent thickness. The collimator also removes the most widely-scattered protons which predominantly contribute to noise in the final image. The collimator effect is shown in the middle column with collimation increasing from top to bottom. As collimation increases, proton transmission from an object is reduced, and contrast is increased. The effect is most pronounced between images acquired with no collimation (where transmission is not overly sensitive to changes in object thickness) and any collimation.

### Effect of Phantom

Different phantoms have different materials and dimensions, thereby providing different levels of contrast. Phantom effect is shown in the middle row. The lead phantom is the most visible, and the water cylinder phantom the least visible. The cylinder phantom is more visible than the Jaszczak water phantom due to the cylinder depths compared to sphere diameters.

### Effect of Contrast Agent

Since proton radiography is a transmission imaging modality, strong differences in proton scatter, a function of density and atomic number  $Z$ , provide greater contrast. The three contrasts (<sup>68</sup>Ga, Au, and water) have different  $Z$  and density contributing to differences in proton scatter. The effect of contrasts are shown on the bottom row (left to right increasing  $Z$ ).

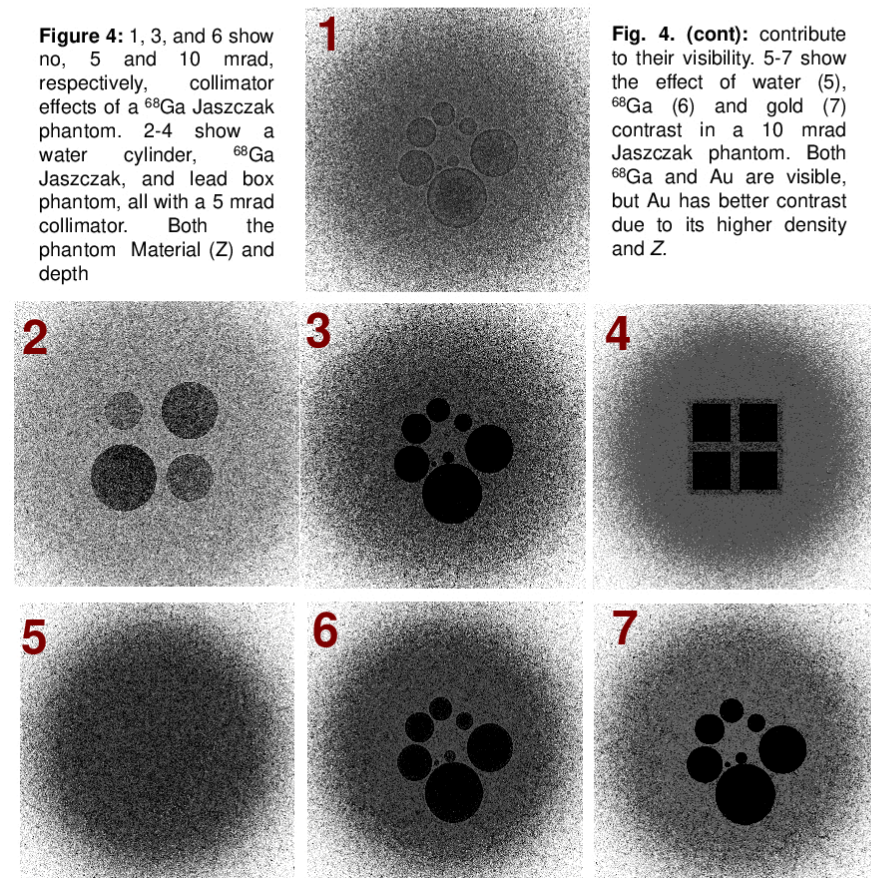


**Figure 4:** 1, 3, and 6 show no, 5 and 10 mrad, respectively, collimator effects of a <sup>68</sup>Ga Jaszczak phantom. 2-4 show a water cylinder, <sup>68</sup>Ga Jaszczak, and lead box phantom, all with a 5 mrad collimator. Both the phantom Material ( $Z$ ) and depth

**Fig. 4. (cont):** contribute to their visibility. 5-7 show the effect of water (5), <sup>68</sup>Ga (6) and gold (7) contrast in a 10 mrad Jaszczak phantom. Both <sup>68</sup>Ga and Au are visible, but Au has better contrast due to its higher density and  $Z$ .

## INNOVATION

While TOPAS has been used in proton therapy plan validation and proton imaging for clinical photon energies up to the typical treatment energy of 230 MeV, it has not been used to simulate proton radiography for high energies, such as the 800 MeV protons used at LANSCE that could also be used for FLASH proton therapy. By creating a user-friendly, open-source tool easily customizable to individual phantoms and positions, TOPAS models could allow users and the medical community to more easily determine the viability of their experiment and make adjustments as needed, as well as compare image results and dose deposition from energies up to 230 MeV to the higher energies investigated here.

## DISCUSSION AND FUTURE WORK

TOPAS provided an effective platform to design Geant4-based Monte Carlo simulations of proton radiography using the full physics list available from Geant4. The results of the simulations with dense, high- $Z$  materials match those seen at pRad: the collimator was shown to have a significant and quantifiable effect on transmission. Without a collimator, transmission was high and also lead to limning (highlighted edges) due to added blur. Adding a collimator makes transmission sensitive to changes in areal density and WEPL. Results shown here demonstrate low contrast using water, indicating that a higher  $Z$  contrast agent would be necessary for proton radiography to differentiate healthy tissue from tumor, both of which would have an approximately identical density and  $Z_{eff}$ .

For the same gold-filled Jaszczak phantom, having no collimator gave 16% transmission through the largest sphere; a 5 mrad collimator gave 0.95% transmission; and a 10 mrad collimator gave 3% transmission. Utilizing an appropriate collimator can make transmission highly sensitive to changes in water thickness: when transmission is  $\sim 50\%$ , a small change in object thickness can result in a large change in transmission and more accurately estimating WEPL. Transmission in the Jaszczak phantoms demonstrated an expected scaling with relation to integrated target density.

Future work will focus on further developing this model and validating these results experimentally using mice with <sup>68</sup>Ga-DOTATATE as the tumor-enhancing contrast agents. <sup>68</sup>Ga-DOTATATE is a PET tracer with a short half-life that decays to Zinc, which may also be visible with proton radiography, thus enabling the evaluation of contrast-enhanced proton radiography for tumor detection. Results of these studies can be confirmed using CT (computed tomography), MRI (magnetic resonance imaging), and PET due to the dual-modality nature of these tracers. In simulations, more accurate phantoms will be created by placing the contrast spheres in a water cylinder, as is done with a real Jaszczak phantom. Additionally, the level of contrast material needed to provide a visible signal will be assessed to determine the minimum amount of contrast agent needed for experimental studies.

## ACKNOWLEDGEMENTS

This work was supported by Los Alamos National Laboratory LDRD under DOE/NNSA contract DE-AC52-06NA25396. This project was also supported in part by the National Physical Sciences Consortium as part of the NPSC Fellowship.

## REFERENCES

- [1] J. Perl, J. Shin, et al., "TOPAS: an innovative proton Monte Carlo platform for research and clinical applications," Medical physics 39, 6818-6837 (2012).
- [2] N. King, E. Ables, et al., "An 800-MeV proton radiography facility for dynamic experiments," Nucl. Instrum. Meth. A 424, 84-91 (1999).
- [3] C.T. Mottershead, J.D. Zumbro, presented at the Part. Accel. Conf., Vancouver, BC, 1997 (unpublished).
- [4] D. Yan, F. Vicini, et al., "Adaptive radiation therapy," Physics in Medicine & Biology 42, 123 (1997).
- [5] Tanabashi, Masaharu, et al. "Review of particle physics." Physical Review D 98.3 (2018): 030001.
- [6] Schaffner, Barbara, and Eros Pedroni. "The precision of proton range calculations in proton radiotherapy treatment planning: experimental verification of the relation between CT-HU and proton stopping power." Physics in Medicine & Biology 43.6 (1998): 1579.
- [7] K. Makino, M. Berz, "Cosy infinity version 9," Nucl. Instrum. Meth. A 558, 346-350 (2006).